

Pectoralis Major — Posterior Deltoid :

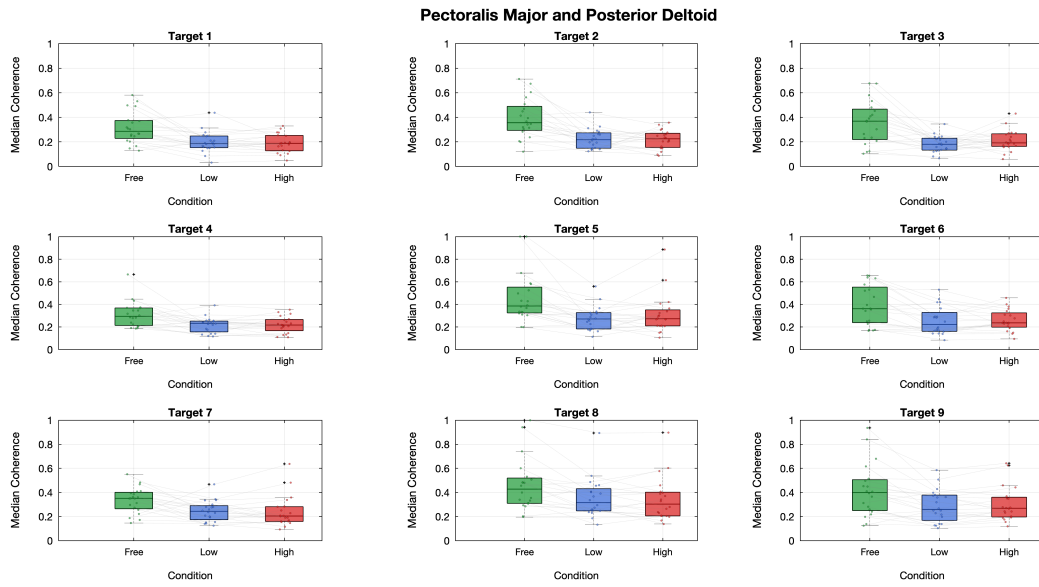


Figure A.11: Pectoralis Major — Posterior Deltoid coherence boxplot.

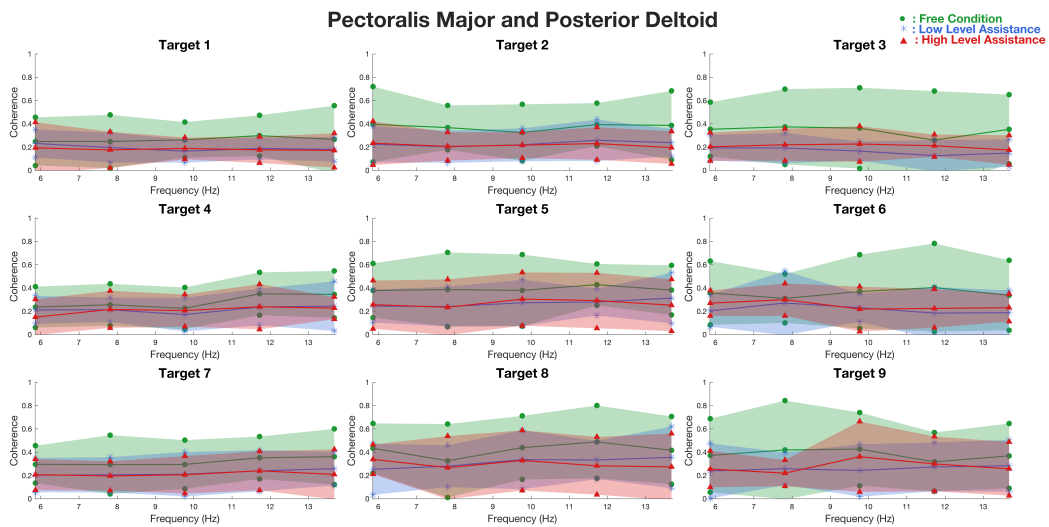


Figure A.12: Pectoralis Major — Posterior Deltoid coherence spectrum.

Middle Trapezius — Pectoralis Major :

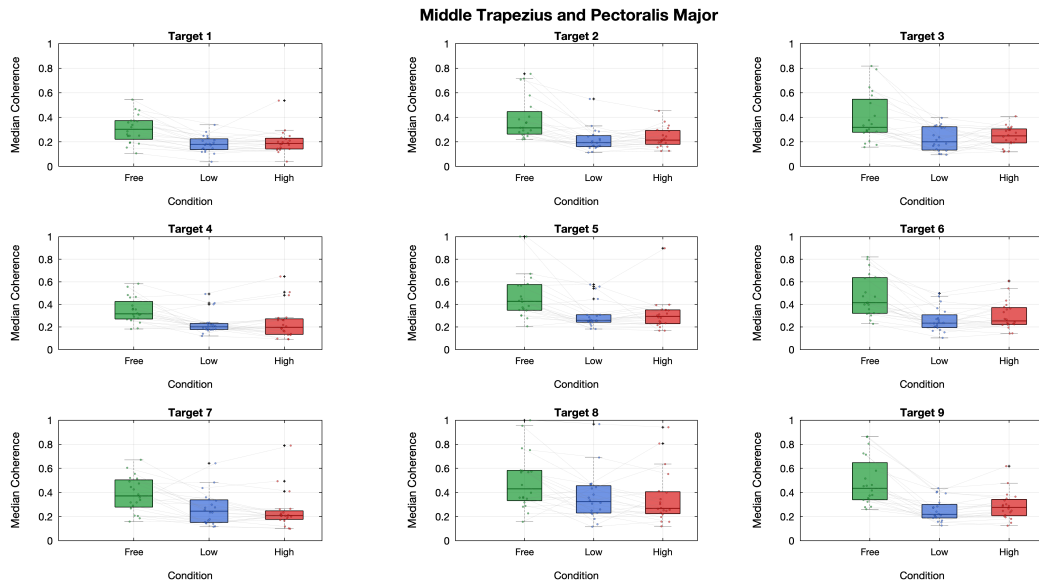


Figure A.13: Middle Trapezius — Pectoralis Major coherence boxplot.

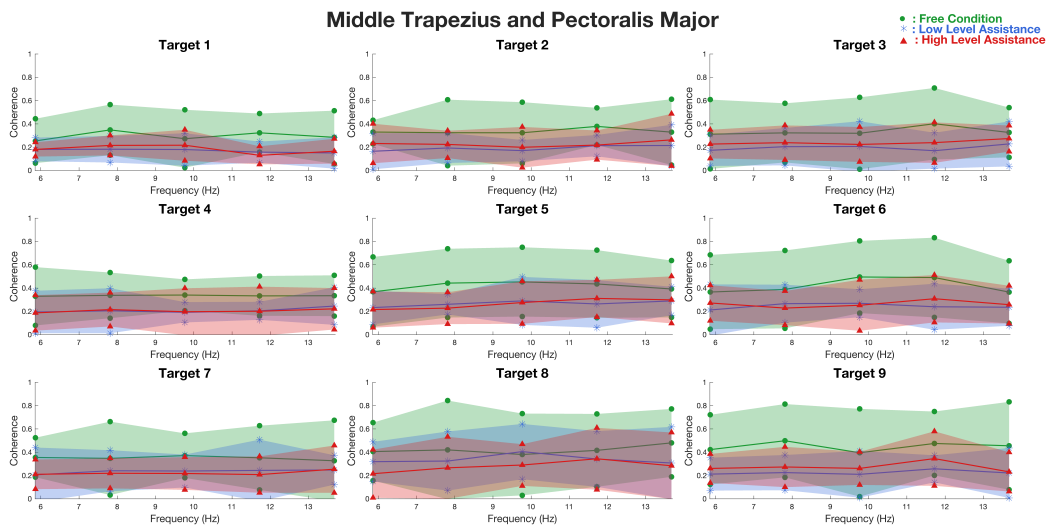


Figure A.14: Middle Trapezius — Pectoralis Major coherence spectrum.

Upper Trapezius — Lower Trapezius :

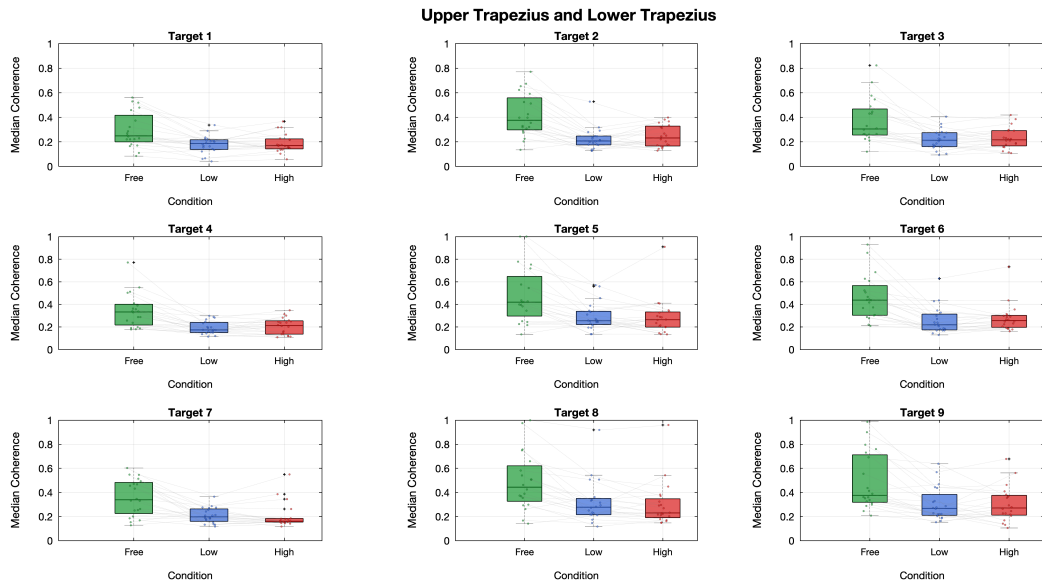


Figure A.15: Upper Trapezius — Lower Trapezius coherence boxplot.

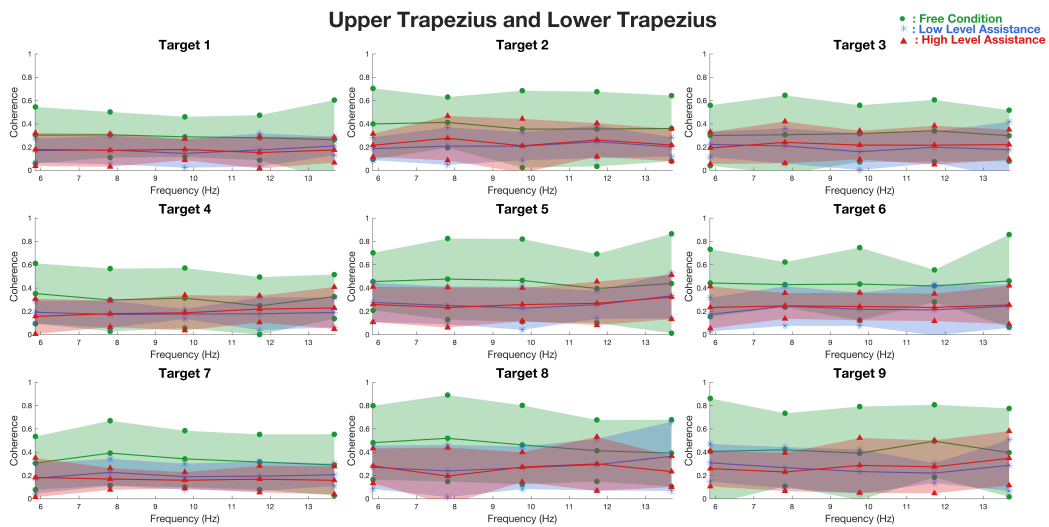


Figure A.16: Upper Trapezius — Lower Trapezius coherence spectrum.

Extensor Carpi Ulnaris — Biceps :

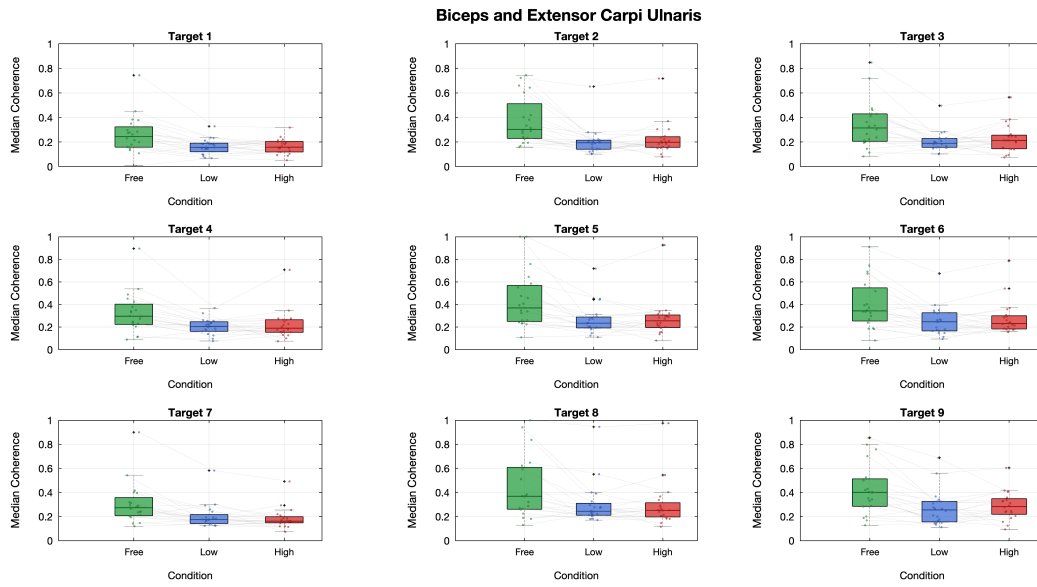


Figure A.17: Extensor Carpi Ulnaris — Biceps coherence boxplot.

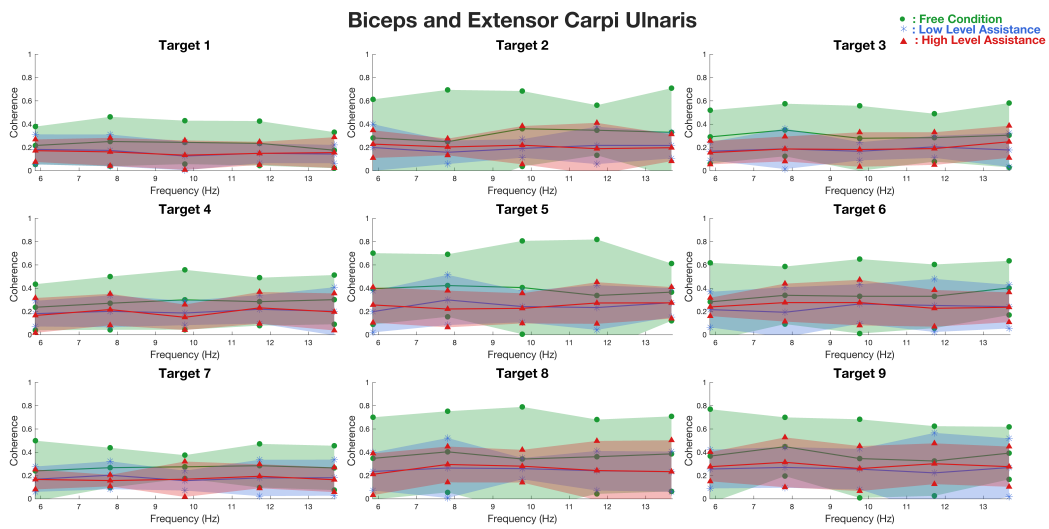


Figure A.18: Extensor Carpi Ulnaris — Biceps coherence spectrum.

A.3 Gamma Band Coherence Analysis

Gamma band oscillations (30–60 Hz) are associated with sensorimotor integration, local cortical processing, and high-frequency synchronization of motor units. In motor control, gamma activity has been associated with precise movement execution, fine motor adjustments, and processing of sensory feedback. Although beta band oscillations (13–30 Hz) reflect common neural drive and broader intermuscular coordination, the coherence of the gamma band is believed to capture higher-frequency synchronization processes and local muscle activation dynamics that arise from central motor commands and peripheral neuromuscular mechanisms.

Gamma band coherence was calculated using analytical methods identical to those used for the primary beta band analysis described in Chapter 2. Coherence estimation employed Welch’s periodogram method with a 512-ms Hamming window, 50% overlap (256 samples), and 512-point FFT at a sampling frequency of 1000 Hz, yielding a frequency resolution of approximately 1.95 Hz.

To ensure adequate spectral sampling of the gamma band, the frequency range was defined as 29.2–60.6 Hz, extending slightly beyond the conventional 30–60 Hz bounds. This extended range captures 17 discrete frequency bins, providing sufficient spectral coverage for reliable coherence estimation and improved visualization.

Gamma band coherence was analyzed across all six muscle pairs, nine targets, and three robotic assistance conditions to explore potential frequency-specific modulation patterns. For each muscle pair, coherence plots display

median values with shaded regions representing interquartile range (IQR) across subjects for each of the nine targets. Similarly, boxplots (Figures) show the distribution of median coherence values for each target, with individual subject data points connected across conditions.

Gamma band coherence exhibited the same qualitative pattern as beta band coherence (Chapter 3): Free condition showed higher coherence values than the assisted conditions, while Low and High assistance levels remained nearly indistinguishable from each other. Specifically:

- The Free condition displayed higher coherence values, but with considerable overlap with the assisted conditions at all frequency points.
- The Low and High assistance conditions showed nearly identical coherence distributions, replicating the beta band observations.
- Boxplot analysis confirmed the consistent $\text{Free} > \text{Low} \approx \text{High}$ trend observed across all nine targets.

In summary, while the gamma band analysis confirmed the general trend of Free higher than Assisted conditions, it did not contribute additional discriminative power or novel findings. This exploratory analysis, together with alpha band results, validates the focus on beta band coherence as the primary biomarker for this application, demonstrating that other frequency bands do not enhance the assessment of robotic assistance effects on neuromuscular coordination.

The following figures present the gamma-band coherence analysis for each muscle pair, with boxplots showing the statistical distribution across targets

Appendix A: Additional and Supplementary Coherence Analyses

and conditions, and frequency-domain coherence spectra with shaded error regions representing the interquartile range across all targets.

Biceps Brachii — Triceps Brachii :

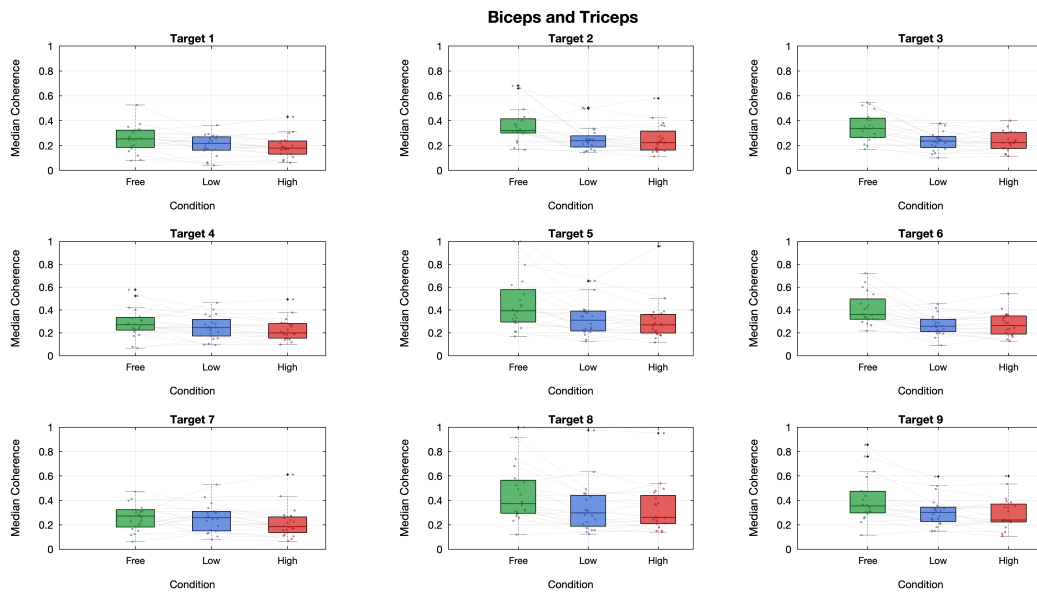


Figure A.19: Biceps — Triceps gamma band coherence boxplot.

Appendix A: Additional and Supplementary Coherence Analyses

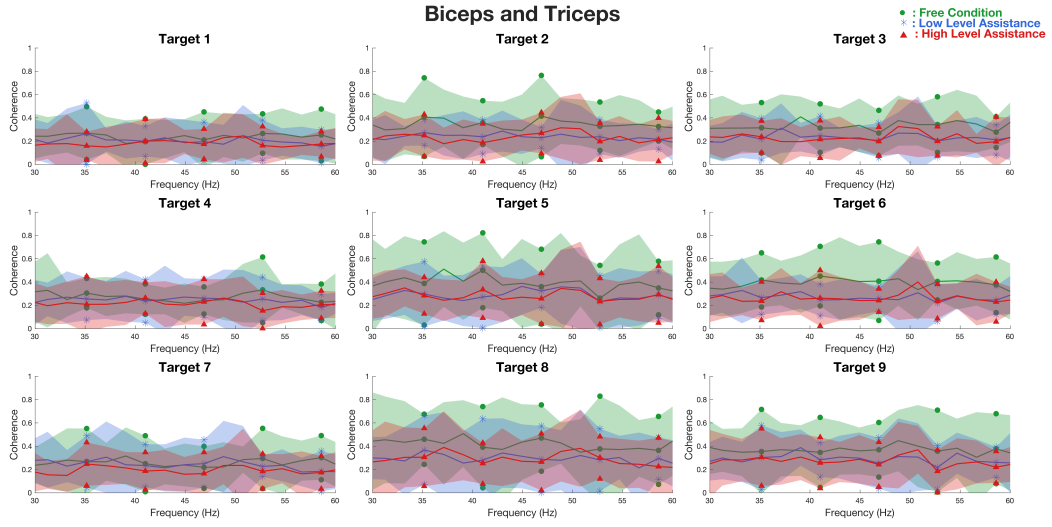


Figure A.20: Biceps — Triceps gamma band coherence frequency spectrum.

Anterior Deltoid — Posterior Deltoid :

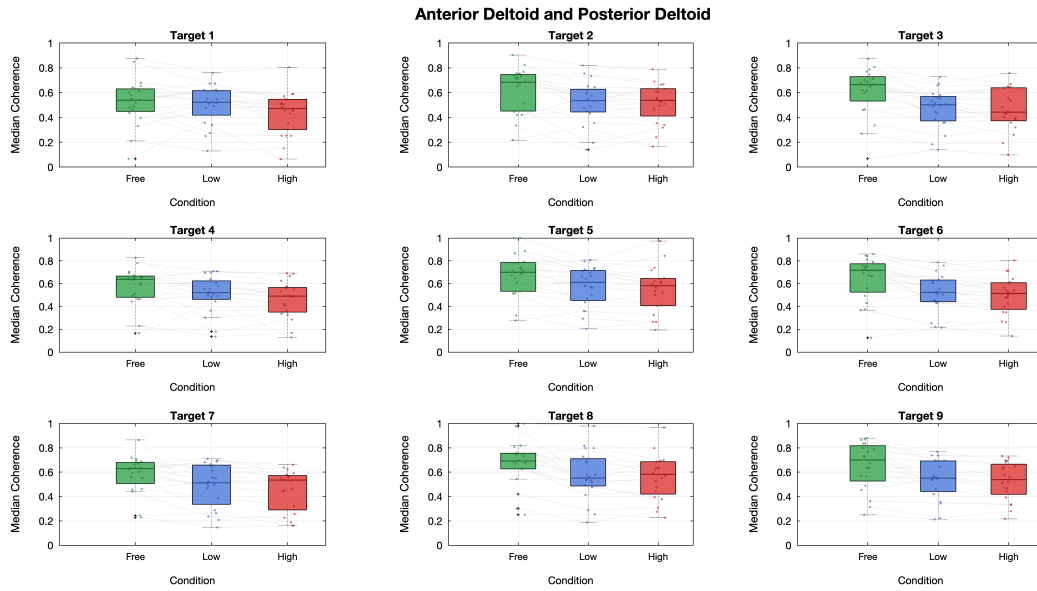


Figure A.21: Anterior Deltoid — Posterior Deltoid coherence boxplot.

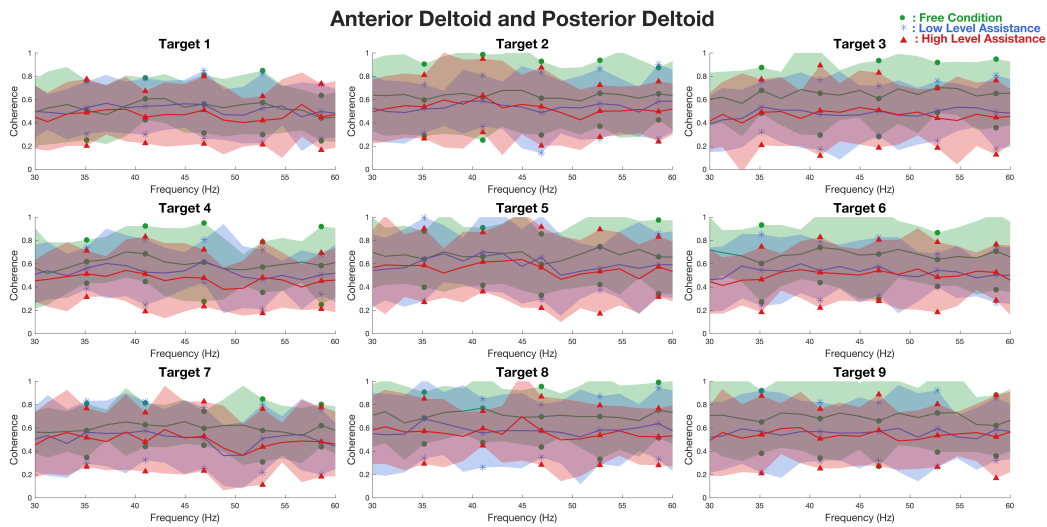


Figure A.22: Anterior Deltoid — Posterior Deltoid coherence spectrum.

Pectoralis Major — Posterior Deltoid :

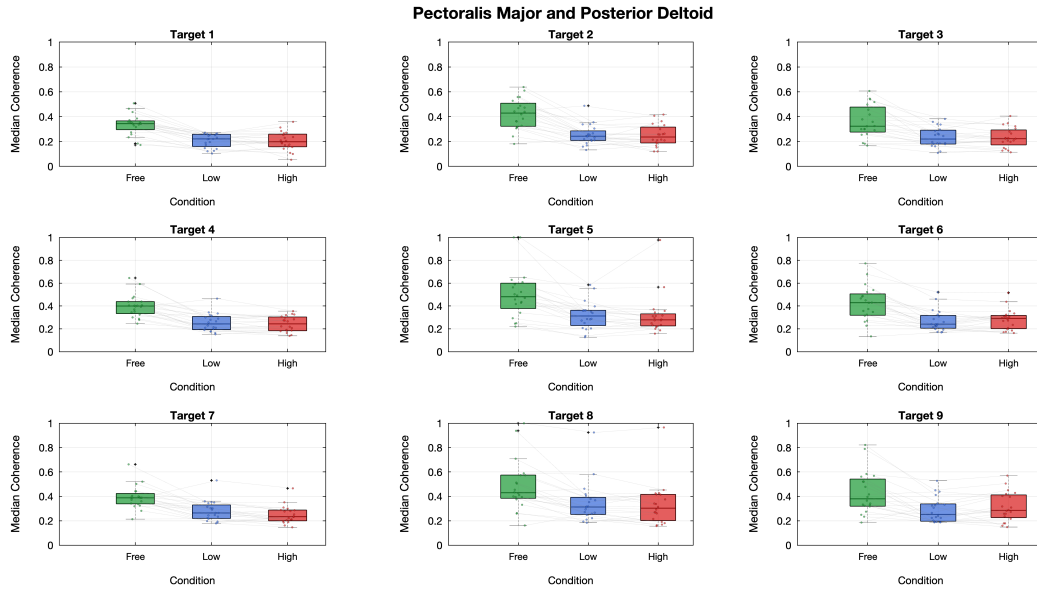


Figure A.23: Pectoralis Major — Posterior Deltoid coherence boxplot.

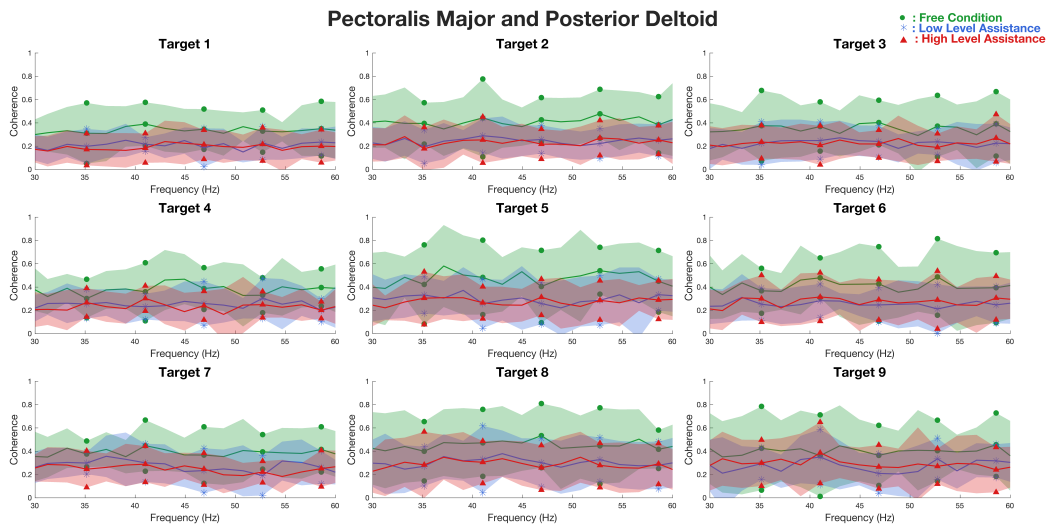


Figure A.24: Pectoralis Major — Posterior Deltoid coherence spectrum.

Middle Trapezius — Pectoralis Major :

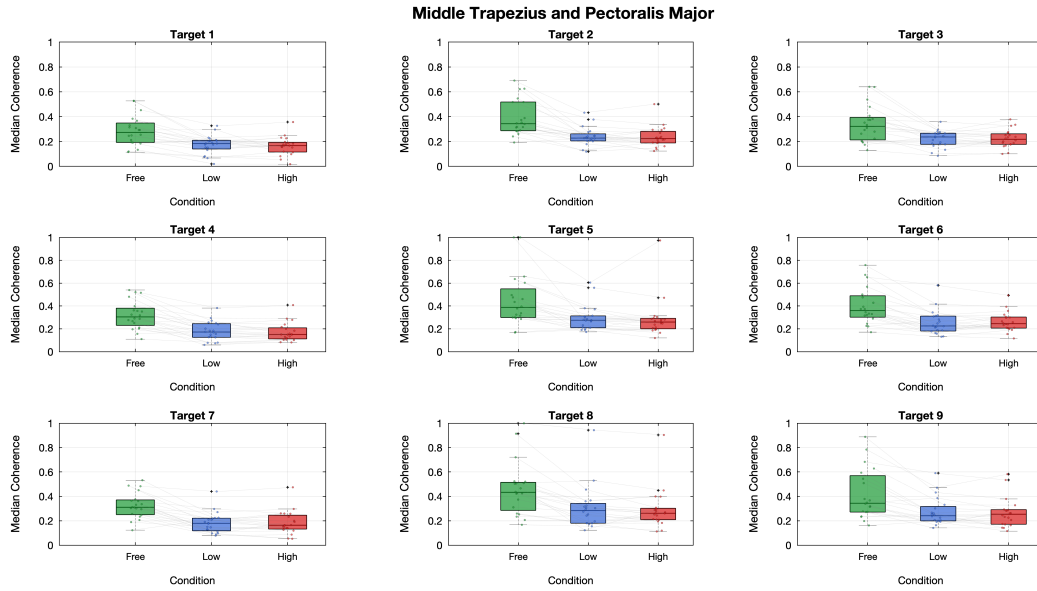


Figure A.25: Middle Trapezius — Pectoralis Major coherence boxplot.

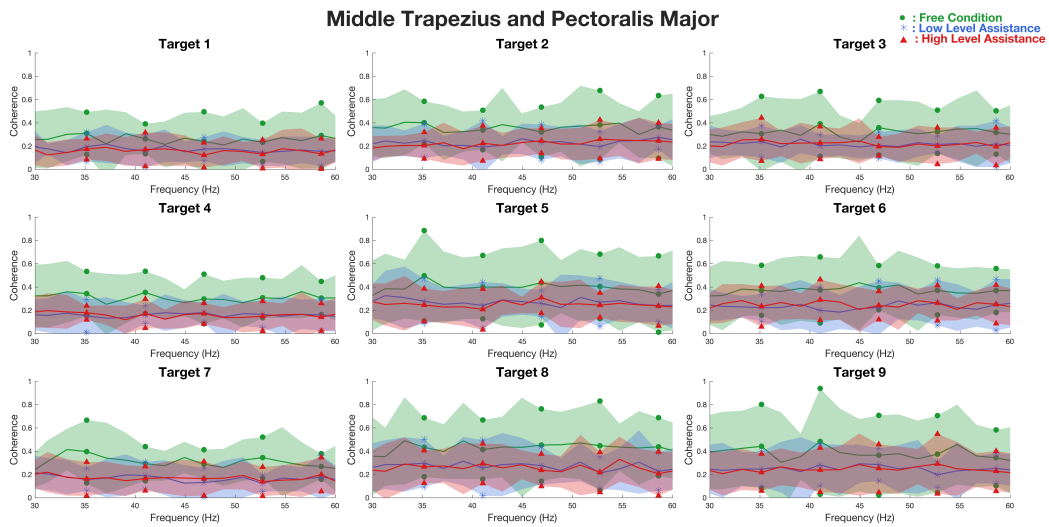


Figure A.26: Middle Trapezius — Pectoralis Major coherence spectrum.

Upper Trapezius — Lower Trapezius :

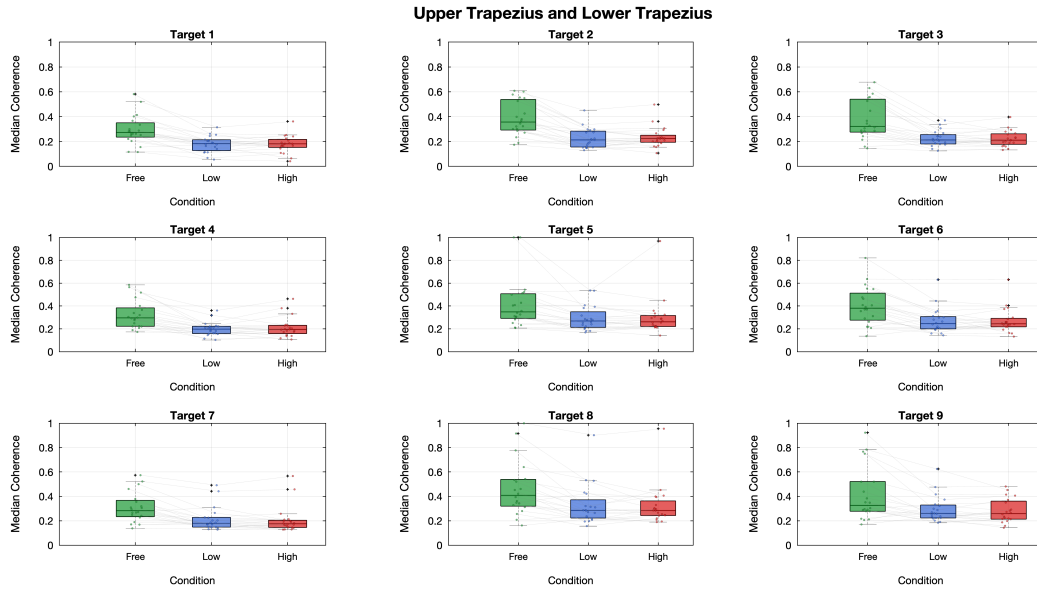


Figure A.27: Upper Trapezius — Lower Trapezius coherence boxplot.

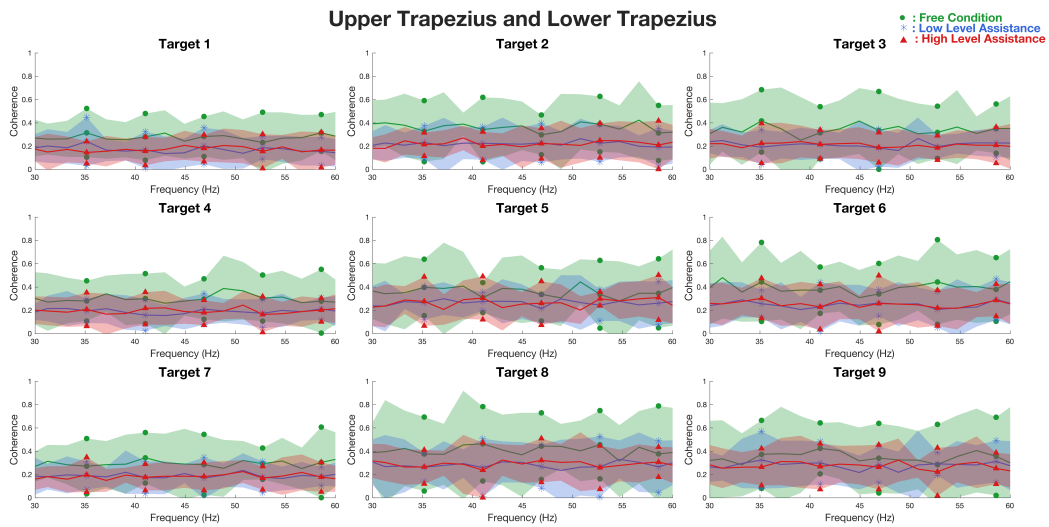


Figure A.28: Upper Trapezius — Lower Trapezius coherence spectrum.

Extensor Carpi Ulnaris — Biceps :

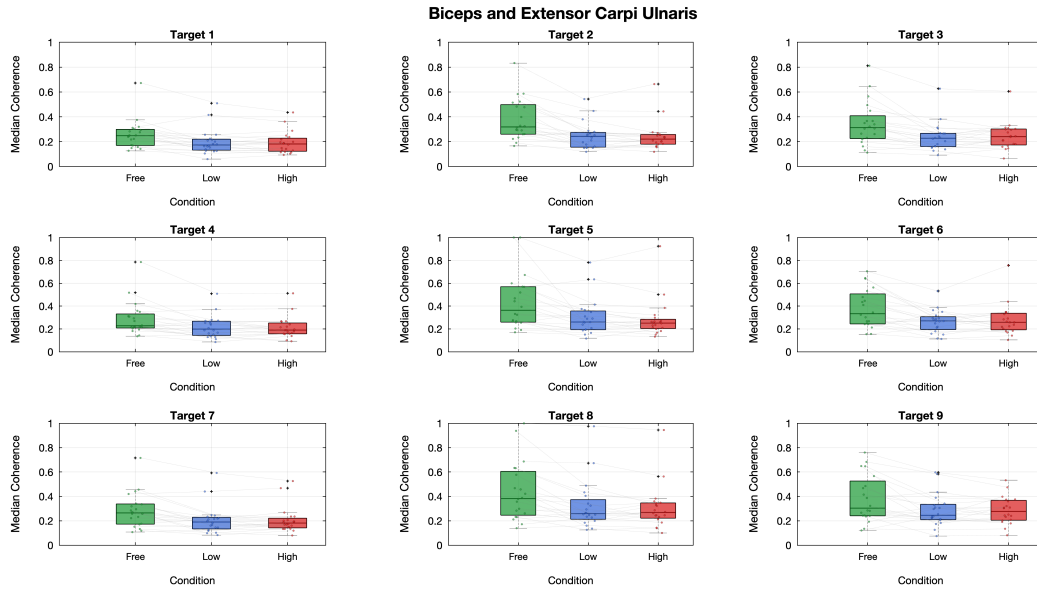


Figure A.29: Extensor Carpi Ulnaris — Biceps coherence boxplot.

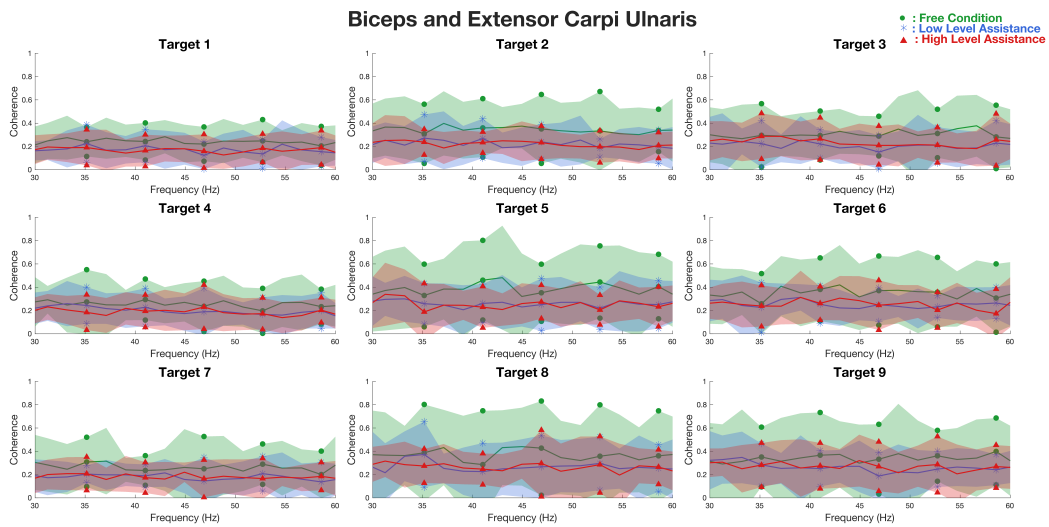


Figure A.30: Extensor Carpi Ulnaris — Biceps coherence spectrum.